Robotics and Autonomous Systems 70 (2015) 145–155

Contents lists available at ScienceDirect

Robotics and Autonomous Systems

journal homepage: www.elsevier.com/locate/robot

Nonlinear control of mobile inverted pendulum

R.M. Brisilla *, V. Sankaranarayanan

Department of Electrical and Electronics Engineering, National Institute of Technology, Tiruchirappalli, India

HIGHLIGHTS

- A single level nonlinear controller is proposed for the point stabilization of MIP.
- Four configuration variables are controlled using two control inputs.
- There is no switching between the controllers.
- Controller is designed using a co-ordinate transformation and feedback linearization.
- The stability of the internal dynamics of the closed loop system is proved.

ARTICLE INFO

Article history:
Received 11 June 2014
Received in revised form
23 January 2015
Accepted 20 February 2015
Available online 4 March 2015

Keywords:
Mobile inverted pendulum (MIP)
Nonlinear control
Underactuated system

ABSTRACT

The mobile inverted pendulum (MIP) is a robotic system with nonholonomic constraint due to no-slip condition imposed on the wheel. In particular, it has four configuration variables to be controlled using only two control inputs. In this paper, we propose a nonlinear control strategy to move the MIP from one point to another point in the configuration space while stabilizing the pendulum. The proposed single level controller is designed using a nonlinear co-ordinate transformation which leads to a simple three step navigation design procedure. The proposed controller stabilizes all four configuration variables without switching between the controllers. Simulation results are presented to validate the proposed technique.

1. Introduction

Two wheeled self balancing robots are used for mobile applications involving narrow spaces and sloped environment. The laboratory version of this robotic system is called as "mobile inverted pendulum". It has two wheels attached to its chassis and a pendulum which can rotate about its wheel axis. The pendulum is attached to the center of mass of the system in an inverted position. This system has nonholonomic[1] constraints due to no slip condition imposed on the wheels and also underactuated.[2] Yamabico Kurara [1], Segway [2] and Joe [3] are some of the existing models of MIP and in particular Segway is commercially available as a human transporter.

Controller design for MIP is a challenging task due to nonholonomic constraints and underactuation. Moreover it has four configuration variables to be controlled with only two control inputs. This system fails to satisfy the necessary condition for asymptotic stabilization of the equilibrium using a continuous control law [4]. The system cannot be fully feedback linearizable and the internal dynamics are nonlinear [5,6]. Many control strategies are developed for MIP in the literature based on the stabilization principle of inverted pendulum [7] and control techniques such as pole placement [3,8], sliding mode [9,10], backstepping [11], Lyapunov redesign [12], adaptive control, fuzzy control [13,14] and neural control [15] have been proposed.

The controllers proposed for MIP in [1,8,9] can perform autonomous navigation whereas in [3] it can track driver's input. As an application of MIP, a baggage transportation system is proposed in [16] by configuring the system into two co-operative subsystems namely, balancing and traveling control subsystem and navigation control subsystem. The robot is stopped at subgoal positions to cancel the posture error due to the linear controller. The controllability and feedback linearizability of MIP are investigated in [6] using nonlinear mathematical model and the authors developed separate two level controllers for stabilizing the MIP, one for tracking orientation and heading speed and the other for position control. However, the position controller fails to reorient the robot to the desired angle and hence the final orientation is achieved

* Corresponding author.
E-mail addresses: brisillamary@gmail.com (R.M. Brisilla), sankariitb@gmail.com (V. Sankaranarayanan).

[1] Nonholonomic constraints are non-integrable and restricts types of motion but not position.

[2] Underactuated systems are defined as system with less number of control inputs than its degrees-of-freedom.

http://dx.doi.org/10.1016/j.robot.2015.02.012
0921-8890/

through an in place rotation using another controller. The problems of model uncertainties of MIP are dealt in [12] and the controller is designed through the combination of time scaling and Lyapunov redesign. The system is time scaled into two subsystems using a delay mechanism and a two level controller is developed to handle the effect of parametric uncertainties and external disturbances.

Other techniques such as neural network [17,18,15,19,20], fuzzy logic [21], neuro-fuzzy [22], energy based controllers [23] and model based controllers [24–27] are also employed for the stabilization of MIP. In [24], velocity control of MIP under uncertainty is investigated using sliding mode control, whereas in [18,17,15], neural adaptive controllers are designed for the trajectory tracking of MIP in uncertain condition. A linear position tracking controller is developed in [25] using a smooth coordinate transformation. Most of the control techniques proposed in the literature concentrate on trajectory tracking with linear controllers and the controller designed for three degrees of freedom point-to-point stabilization needs switching between the controllers [28]. Global stabilization of MIP with a single level controller without any switching between the controllers is still a challenging task whereas the pendulum on a cart system which is also underactuated like MIP is stabilized using a single controller in [29] and its global stabilization is obtained in [30] using combination of control techniques namely, input–output linearization, energy control, and singular perturbation theory.

This paper proposes a single layer nonlinear controller to move the MIP from any initial position and orientation to any desired position and orientation while stabilizing the pendulum (four degrees of freedom) using only two controllers without any switching between the controllers. First the nonlinear dynamic model of the system is transformed to a new co-ordinate which simplifies the system model and helps to design the controller. Further, the system is partially feedback linearized to design two independent controllers to move the robot from any initial position and orientation to the desired position and orientation while stabilizing the pendulum. Contrary to the previous control approaches, the controller designed in this paper accomplishes a series of motion tasks such as homing, moving toward the target and stopping at the desired point in a required orientation without any halt during the motion. The effectiveness of the controller is validated through numerical simulations.

The rest of the paper is organized as follows. In Section 2, the dynamic model of the system is presented. The state transformation, internal dynamics and the controller design for point to point stabilization of MIP with stability analysis of closed loop system are illustrated in Section 3. Section 4 outlines the effectiveness of the proposed controller through simulation results. Finally, Section 5 presents concluding remarks.

2. Mathematical model of mobile inverted pendulum

The structure of MIP consists of a pendulum that can rotate about its pivot, which is attached to the center of the line joining the two wheels provided on the chassis as shown in Fig. 1. The system has four degrees of freedom $(x,\ y,\ \theta,\ \alpha)$; $x,\ y$ are position in x–y plane, θ is the orientation angle and α is the pendulum angle. The position of the robot is controlled through two independent motors which drive the wheels. The system parameters are given in Table 1.

We define three co-ordinate frames each with three orthogonal axes, namely inertial frame $(X,\ Y,\ Z)$, vehicle co-ordinate frame $(X_v,\ Y_v,\ Z_v)$ and pendulum body co-ordinate frame $(X_b,\ Y_b,\ Z_b)$. Inertial frame is the reference frame and the point 'O' which is defined by the position vector $(x,\ y,\ R)^T$ in this frame is located at the center of the line joining the two wheels. The vehicle co-ordinate frame is introduced to represent the orientation angle

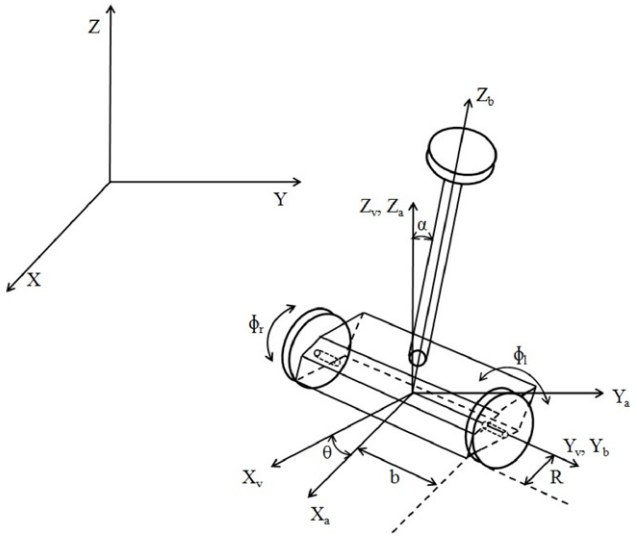

Fig. 1. Schematic of mobile inverted pendulum.

$\theta = \angle(X,\ X_v)$ about the Z axis and the pendulum body co-ordinate frame is attached to the pendulum body such that the pendulum angle $\alpha = \angle(Z, Z_b)$. The position of the center of mass of the pendulum body about the body co-ordinate frame is given by the vector $(0,\ 0,\ c_z)$. The co-ordinates $(X_a,\ Y_a,\ Z_a)$ represents an arbitrary frame that is parallel to the inertial frame and attached to the point 'O'. The position of the MIP in the inertial frame can be obtained by rotating the X_a axis by an angle θ about Z axis and Z_a axis by an angle α about the Y_v axis.

The state-space model of MIP using the following assumptions:

(1) the robot undergoes motion on a horizontal surface.
(2) the wheels do not tilt away from the vertical and is always in contact with a point on the surface.
(3) the model does not account for the friction and uncertainties.

is written as

$$\dot{\mathbf{x}} = f(\mathbf{x}) + g_1(\mathbf{x})\tau_r + g_2(\mathbf{x})\tau_l \tag{1}$$

where, $\mathbf{x} = \begin{pmatrix} x & y & \theta & \alpha & \dot{\alpha} & v & \dot{\theta} \end{pmatrix}^T$, τ_r and τ_l represent the torques applied to right and left wheels of robot. The drift vector field $f(\mathbf{x})$ and the control vector fields $g_1(\mathbf{x})$, $g_2(\mathbf{x})$ are given by

$$f(\mathbf{x}) = \begin{pmatrix} v\cos\theta \\ v\sin\theta \\ \dot{\theta} \\ \dot{\alpha} \\ f_5(\alpha, \dot{\alpha}, \dot{\theta}) \\ f_6(\alpha, \dot{\alpha}, \dot{\theta}) \\ f_7(\alpha, \dot{\alpha}, \dot{\theta}) \end{pmatrix}; \quad g_1(\mathbf{x}) = \begin{pmatrix} 0 \\ 0 \\ 0 \\ 0 \\ -\dfrac{g_5(\alpha)}{RT_1(\alpha)} \\ \dfrac{g_6(\alpha)}{RT_1(\alpha)} \\ \dfrac{b}{RT_2(\alpha)} \end{pmatrix}; \quad g_2(\mathbf{x}) = \begin{pmatrix} 0 \\ 0 \\ 0 \\ 0 \\ -\dfrac{g_5(\alpha)}{RT_1(\alpha)} \\ \dfrac{g_6(\alpha)}{RT_1(\alpha)} \\ -\dfrac{b}{RT_2(\alpha)} \end{pmatrix}. \tag{2}$$

Table 1
List of symbols.

M_b	Mass of the pendulum body
M_w	Mass of each wheel
R	Radius of wheel
$2b$	Distance between the two wheels
g	Acceleration due to gravity
$(0, 0, c_z)^T$	Center of mass of pendulum body with respect to pendulum body coordinate frame
I_{wa}	Moment of inertia of each wheel about its roll axis
$I_b = \text{diag}(I_x I_y I_z)$	Moment of inertia matrix of pendulum body with respect to its center of mass
I_{wd}	Moment of inertia of each wheel about a diameter
ϕ_r, ϕ_l	Angle of rotation of right and left wheel of MIP
τ_r, τ_l	Torque applied to the right and left wheel of MIP
v	Linear velocity

The functions appearing in the vector fields (2) are defined as follows.

$$
\begin{aligned}
T_1(\alpha) &= b_2 b_3 - b_5^2 \cos^2(\alpha)\\
T_2(\alpha) &= b_4 + b_1 \sin^2 \alpha\\
g_5(\alpha) &= b_3 R + b_5 \cos\alpha\\
g_6(\alpha) &= b_2 + R b_5 \cos\alpha\\
f_5(\alpha, \dot\alpha, \dot\theta) &= \frac{\sin 2\alpha (b_3 b_1 \dot\theta^2 - b_5^2 \dot\alpha^2) + 2 b_5 b_3 g \sin\alpha}{2(b_2 b_3 - b_5^2 \cos^2\alpha)}\\
f_6(\alpha, \dot\alpha, \dot\theta) &= \frac{\sin 2\alpha (-b_1 b_5 \dot\theta^2 \cos\alpha - b_5^2 g) + 2 b_2 b_5 \dot\alpha^2 \sin\alpha}{2(b_2 b_3 - b_5^2 \cos^2\alpha)}\\
f_7(\alpha, \dot\alpha, \dot\theta) &= \frac{-b_1 \dot\alpha \dot\theta \sin 2\alpha}{b_4 + b_1 \sin^2\alpha}.
\end{aligned}
$$

Assume that, the parameters of MIP are designed to satisfy the following conditions

$$
\begin{aligned}
T_1(\alpha) &> 0 \quad \forall \alpha \in A_s\\
T_2(\alpha) &> 0 \quad \forall \alpha \in A_s\\
g_5(\alpha) &> 0 \quad \forall \alpha \in A_s\\
g_6(\alpha) &> 0 \quad \forall \alpha \in A_s
\end{aligned}
$$

where $A_s = \{-\frac{\pi}{2} < \alpha < \frac{\pi}{2}\}$.

The parameters b_1, b_2, b_3, b_4 and b_5 are given by,

$$
\begin{aligned}
b_1 &= M_b c_z^2 + I_x - I_z\\
b_2 &= M_b c_z^2 + I_y\\
b_3 &= \frac{M_b R^2 + 2(I_{wa} + M_w R^2)}{R^2}\\
b_4 &= \frac{R^2(I_z + 2I_{wd} + 2b^2 M_w) + 2b^2 I_{wa}}{R^2}\\
b_5 &= M_b c_z.
\end{aligned} \tag{3}
$$

The equilibrium configuration is $\xi \triangleq \{x, y, \theta, 0, 0, 0, 0 : (x, y, \theta) \in R^2 \times S^1\}$. The MIP is not linearly controllable about any of its equilibrium point. But, the system is strongly accessible and small time locally controllable [6].

3. Controller design

The control objective is to steer the robot from any initial point $\mathbf{x}(0)$ to the desired equilibrium point while stabilizing the pendulum. Without loss of generality, the point to point control problem can be considered as the stabilization problem of system (1) around the origin. We used the following state transformation [31] to derive a simplified model which helps in designing the controller.

$$
\begin{aligned}
z_1 &= \theta\\
z_2 &= x\cos\theta + y\sin\theta\\
z_3 &= x\sin\theta - y\cos\theta\\
z_4 &= \dot\theta\\
z_5 &= v\\
z_6 &= \alpha\\
z_7 &= \dot\alpha.
\end{aligned} \tag{4}
$$

System (1) after the state transformation (4) is given by,

$$
\begin{aligned}
\dot z_1 &= z_4\\
\dot z_2 &= z_5 - z_3 z_4\\
\dot z_3 &= z_4 z_2\\
\dot z_4 &= -\frac{b_1 z_7 z_4 \sin 2z_6}{b_4 + b_1 \sin^2 z_6} + \frac{b}{R(b_4 + b_1 \sin^2 z_6)}(\tau_r - \tau_l)\\
\dot z_5 &= \frac{(\sin 2z_6)(-b_1 b_5 z_4^2 \cos z_6 - b_5^2 g) + 2 b_2 b_5 z_7^2 \sin z_6}{2(b_2 b_3 - b_5^2 \cos^2 z_6)}\\
&\quad + \frac{b_2 + R b_5 \cos z_6}{R(b_2 b_3 - b_5^2 \cos^2 z_6)}(\tau_r + \tau_l)\\
\dot z_6 &= z_7\\
\dot z_7 &= \frac{\sin 2z_6 (b_3 b_1 z_4^2 - b_5^2 z_7^2) + 2 b_5 b_3 g \sin z_6}{2(b_2 b_3 - b_5^2 \cos^2 z_6)}\\
&\quad - \frac{b_3 R + b_5 \cos z_6}{R(b_2 b_3 - b_5^2 \cos^2 z_6)}(\tau_r + \tau_l)
\end{aligned}
$$

and using the following input transformation,

$$
\begin{aligned}
u_1 &= -\frac{b_1 z_7 z_4 \sin 2z_6}{b_4 + b_1 \sin^2 z_6} + \frac{b}{R(b_4 + b_1 \sin^2 z_6)}(\tau_r - \tau_l)\\
u_2 &= \frac{\sin 2z_6 (b_3 b_1 z_4^2 - b_5^2 z_7^2) + 2 b_5 b_3 g \sin z_6}{2(b_2 b_3 - b_5^2 \cos^2 z_6)}\\
&\quad - \frac{b_3 R + b_5 \cos z_6}{R(b_2 b_3 - b_5^2 \cos^2 z_6)}(\tau_r + \tau_l)
\end{aligned} \tag{5}
$$

the state equations of the system becomes

$$
\begin{aligned}
\dot z_1 &= z_4\\
\dot z_2 &= z_5 - z_3 z_4\\
\dot z_3 &= z_4 z_2\\
\dot z_4 &= u_1\\
\dot z_5 &= \frac{(\sin 2z_6)(-b_1 b_5 z_4^2 \cos z_6 - b_5^2 g) + 2 b_2 b_5 z_7^2 \sin z_6}{2(b_2 b_3 - b_5^2 \cos^2 z_6)}\\
&\quad + \left(\frac{b_2 + R b_5 \cos z_6}{b_3 R + b_5 \cos z_6}\right)\\
&\quad \times \left(\frac{\sin 2z_6 (b_3 b_1 z_4^2 - b_5^2 z_7^2) + 2 b_5 b_3 g \sin z_6}{2(b_2 b_3 - b_5^2 \cos^2 z_6)} - u_2\right)\\
\dot z_6 &= z_7\\
\dot z_7 &= u_2.
\end{aligned} \tag{6}
$$

The system in (6) is in partial feedback linearized form.

Further system (6) can be written in '$\mathcal{Z}$' co-ordinate as

$$
\dot{\mathcal{Z}} = \mathcal{F}(\mathcal{Z}) + \mathcal{G}_1(\mathcal{Z}) u_1 + \mathcal{G}_2(\mathcal{Z}) u_2 \tag{7}
$$

where,

$$
\mathcal{Z} = \begin{pmatrix} z_1 & z_2 & z_3 & z_4 & z_5 & z_6 & z_7 \end{pmatrix}^T
$$

$$\mathcal{F}(\mathcal{Z}) = \begin{pmatrix} z_4 \\ z_5 - z_3 z_4 \\ z_4 z_2 \\ 0 \\ f_z(z_4, z_6, z_7) \\ z_7 \\ 0 \end{pmatrix}; \quad \mathcal{G}_1(\mathcal{Z}) = \begin{pmatrix} 0 \\ 0 \\ 0 \\ 1 \\ 0 \\ 0 \\ 0 \end{pmatrix}; \quad \mathcal{G}_2(\mathcal{Z}) = \begin{pmatrix} 0 \\ 0 \\ 0 \\ 0 \\ -f_u(z_6) \\ 0 \\ 1 \end{pmatrix}. \tag{8}$$

The functions appearing in the vector fields (8) are defined as follows.

$$f_z(z_4, z_6, z_7) = \frac{(\sin 2z_6)(-b_1 b_5 z_4^2 \cos z_6 - b_5^2 g) + 2b_2 b_5 z_7^2 \sin z_6}{2(b_2 b_3 - b_5^2 \cos^2 z_6)} + \left(\frac{b_2 + R b_5 \cos z_6}{b_3 R + b_5 \cos z_6}\right) \times \left(\frac{\sin 2z_6 (b_3 b_1 z_4^2 - b_5^2 z_7^2) + 2b_5 b_3 g \sin z_6}{2(b_2 b_3 - b_5^2 \cos^2 z_6)}\right)$$

$$f_u(z_6) = \left(\frac{b_2 + R b_5 \cos z_6}{b_3 R + b_5 \cos z_6}\right).$$

3.1. Internal dynamics of MIP

Consider the system in (7) with the following output equations

$$\begin{aligned} y_1 &= z_3 \\ y_2 &= z_6. \end{aligned} \tag{9}$$

The zero dynamics of the system (7) can be obtained by making the output equations in (9) identically equal to zero [32,33] and it can be written as $y_1 = 0,\ \dot{y}_1 = 0,\ \ddot{y}_1 = 0,\ y_2 = 0,\ \dot{y}_2 = 0,\ \ddot{y}_2 = 0$.

Now, the zero dynamics can be expressed as

$$\begin{aligned} \dot{z}_3 &= z_4 z_2 = 0 \\ \ddot{z}_3 &= z_4(z_5 - z_3 z_4) + z_2 u_1 = 0 \\ \dot{z}_6 &= z_7 = 0 \\ \ddot{z}_6 &= \dot{z}_7 = u_2 = 0. \end{aligned} \tag{10}$$

The zero dynamics results in $z_3 = 0,\ z_4 = 0,\ \dot{z}_4 = u_1 = 0,\ z_6 = 0,\ z_7 = 0,\ \dot{z}_7 = u_2 = 0$. By substituting this condition in the remaining state equations in (7) we obtain the internal dynamics as follows.

$$\begin{aligned} \dot{z}_1 &= 0 \\ \dot{z}_2 &= z_5 \\ \dot{z}_5 &= 0. \end{aligned} \tag{11}$$

The solution for the internal dynamics (11) can be expressed as

$$\begin{aligned} z_1 &= c_1 \\ z_2 &= z_5 t + c_2 \\ z_5 &= c_5 \end{aligned} \tag{12}$$

where $c_1,\ c_2, c_5 \in R$. Eqs. (12) shows that, the internal dynamics of the system (7) is unstable.

The controller design for MIP in this brief is similar to [34] in which the authors proposed a switched controller to stabilize the mobile robot using three stages namely home toward the target position, move to the target position and then rotate to the desired orientation. The system considered in [34] has 3 degrees-of-freedom (DOF) and stabilized by two control inputs using a sequential switched control strategy. One of the control input is used for orientation control and the other for pure forward motion. The orientation control is inactive when pure forward motion control is applied and vice-versa.

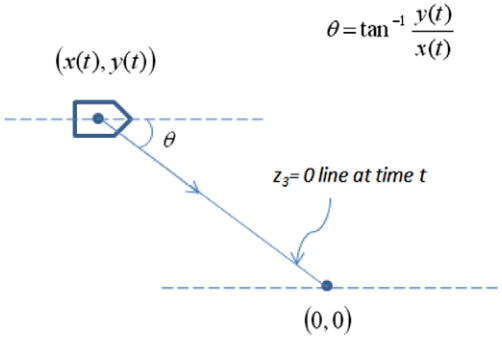

Fig. 2. Homing of MIP toward the target.

The controller proposed to stabilize the mobile robot [34] cannot be applied directly to stabilize the MIP since it has four DOF and two control inputs. We modify the control law proposed in [34] such that both the controllers are active during the entire navigation so that the system finally reaches the desired equilibrium. To proceed with the above idea system (7) is divided into the following three subsystems.

$$\begin{aligned} \dot{z}_1 &= z_4 \\ \dot{z}_4 &= u_1 \end{aligned} \tag{13a}$$

$$\begin{aligned} \dot{z}_6 &= z_7 \\ \dot{z}_7 &= u_2 \end{aligned} \tag{13b}$$

$$\begin{aligned} \dot{z}_2 &= z_5 - z_3 z_4 \\ \dot{z}_5 &= f_z(z_4, z_6, z_7) - f_u(z_6) u_2. \end{aligned} \tag{13c}$$

Note that, the orientation of the MIP is directly controlled through subsystem (13a) and the pendulum angle is directly controlled through subsystem (13b).

3.2. Homing toward the target

The controller design starts with the three stage approach proposed in [34]. The main aim of homing control is to rotate the robot to the target position such that, the robot has to move to the target position along the straight line connecting the initial point and the final point as depicted in Fig. 2. In state-space it is equivalent to stabilizing the state z_3.

Consider the following equation

$$z_3 = x \sin\theta - y \cos\theta.$$

The state z_3 can be made '0' by setting the value of

$$\theta = \tan^{-1}\left(\frac{y}{x}\right). \tag{14}$$

This task can be performed by controlling the θ dynamics through the subsystem (13a)

$$\begin{aligned} \dot{z}_1 &= z_4 \\ \dot{z}_4 &= u_1. \end{aligned}$$

In the original co-ordinate the robot rotates to align with a straight line connecting the initial and final points as shown in Fig. 2. This control scheme is named as "*Homing*" as mentioned

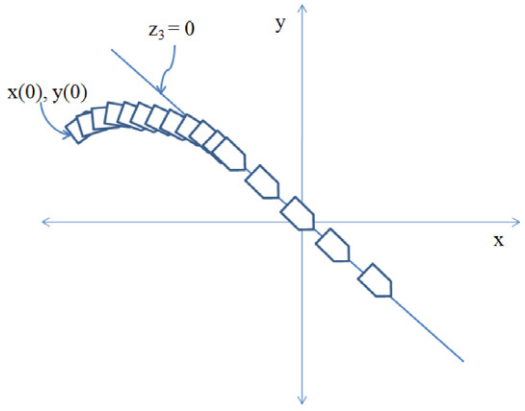

Fig. 3. The trajectory followed by the MIP, when it aligns with the line $z_3 = 0$.

in [34], however the posture in case of MIP is changing, due to the stabilization of pendulum through subsystem (13b). Hence the desired θ to make $z_3 = 0$ is also varying and it is shown in Fig. 3.

$$\theta(t) = \tan^{-1}\left(\frac{y(t)}{x(t)}\right). \tag{15}$$

The value of $\theta(t)$ in (15) becomes indeterminate when $x = 0$, $y = 0$ simultaneously. This problem can be handled by defining $\theta(t)$ as follows

$$\theta(t) = \tan^{-1}\left(\frac{y(t)}{x(t) + \left(1 - \text{sign}\left(x(t)^2 + y(t)^2\right)\right)}\right). \tag{16}$$

We apply the following controller to align the robot to $z_3 = 0$ line which results in $z_1 = z_{1r}(t)$.

$$u_1 = -k_1\left(z_1 - z_{1r}(t)\right) - k_2 z_4 \tag{17a}$$

where $z_{1r}(t) = \theta(t)$.

The stabilizing controller for pendulum is

$$u_2 = -k_3 z_6 - k_4 z_7 \tag{17b}$$

where $k_1,\ k_2,\ k_3,\ k_4$ are positive.

The closed loop system with the control law (17) is

$$\begin{aligned}
\dot{z}_1 &= z_4\\
\dot{z}_2 &= z_5 - z_3 z_4\\
\dot{z}_3 &= z_4 z_2\\
\dot{z}_4 &= -k_1(z_1 - z_{1r}) - k_2 z_4\\
\dot{z}_5 &= \frac{(\sin 2z_6)(-b_1 b_5 z_4^2 \cos z_6 - b_5^2 g) + 2b_2 b_5 z_7^2 \sin z_6}{2(b_2 b_3 - b_5^2 \cos^2 z_6)}\\
&\quad + \frac{b_2 + R b_5 \cos z_6}{b_3 R + b_5 \cos z_6}\\
&\quad \times \left(\frac{\sin 2z_6 (b_3 b_1 z_4^2 - b_5^2 z_7^2) + 2b_5 b_3 g \sin z_6}{2(b_2 b_3 - b_5^2 \cos^2 z_6)}\right)\\
&\quad - \frac{b_2 + R b_5 \cos z_6}{b_3 R + b_5 \cos z_6}(-k_3 z_6 - k_4 z_7)\\
\dot{z}_6 &= z_7\\
\dot{z}_7 &= -k_3 z_6 - k_4 z_7.
\end{aligned} \tag{18}$$

The controller u_1 in (17a) stabilizes z_1 to the target orientation z_{1r} and hence $z_3 = z_4 \to 0$. At the same time the controller u_2 in (17b) stabilizes z_6 and z_7 to zero.

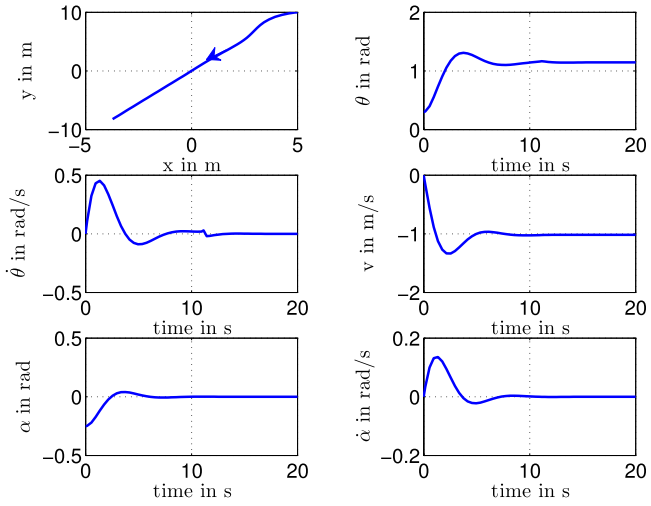

Fig. 4. Response of homing control when the MIP is in quadrant I.

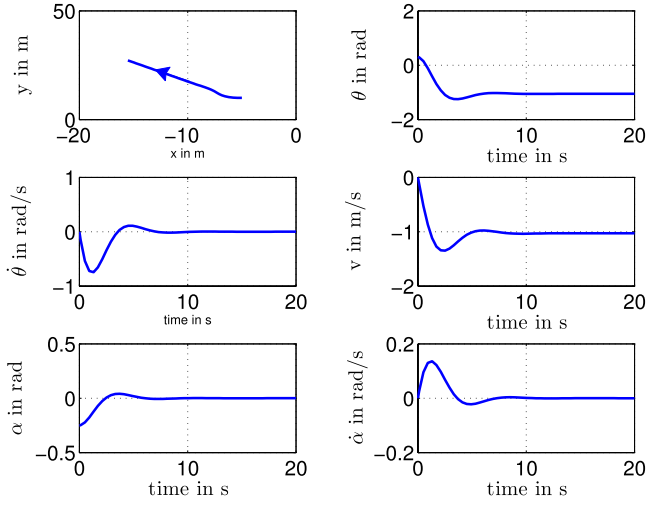

Fig. 5. Response for homing control when the MIP is in quadrant II.

Now, consider the subsystem (13c)

$$\begin{aligned}
\dot{z}_2 &= z_5 - z_3 z_4\\
\dot{z}_5 &= f_z(z_4, z_6, z_7) - f_u(z_6) u_2.
\end{aligned} \tag{19}$$

When $z_3 = z_4 = z_6, z_7 = 0$, (13c) becomes

$$\begin{aligned}
\dot{z}_2 &= z_5\\
\dot{z}_5 &= 0
\end{aligned} \tag{20}$$

and hence $z_5 = c_1, z_2 = c_1 t + c_2$.

The robot moves along a line passing through the origin. However this control action may not drive the robot toward the origin all the time. This strategy is simulated and the results are presented in Figs. 4–7.

3.3. Pedaling action of MIP

The pedaling action of MIP is explained in this section which is used further to modify the controller to stabilize the MIP. The pendulum can be used as a pedal to move the MIP along the direction of pendulum as shown in Fig. 8.

Consider the subsystem (13a)

$$\begin{aligned}
\dot{z}_1 &= z_4\\
\dot{z}_4 &= u_1
\end{aligned}$$

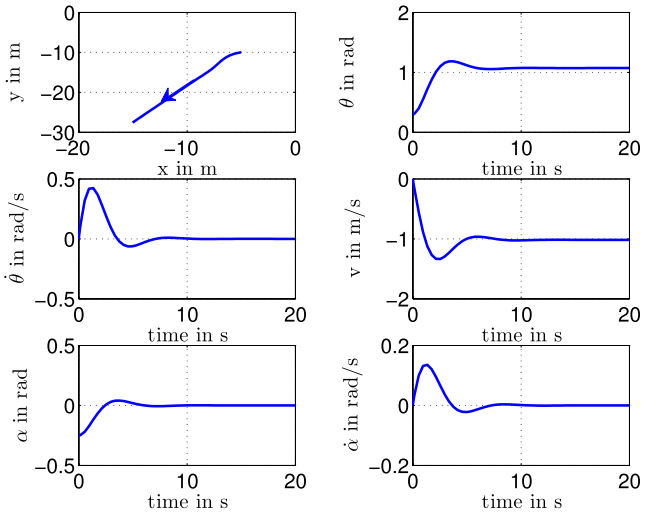

Fig. 6. Response for homing control when the MIP is in quadrant III.

and (13b)

$$\dot{z}_6 = z_7$$
$$\dot{z}_7 = u_2.$$

Assume that the MIP is not rotating about 'Z' axis and hence $u_1 = z_4 = 0$.

Consider the following control law, for the subsystem (13b),

$$u_2 = -k_3 z_6 - k_4 z_7 - \mathcal{K} \tag{21}$$

where $k_3,\ k_4, \mathcal{K} \in \mathcal{R}$ are controller gains and $k_3,\ k_4$ are positive.

This control law regulates the pendulum angle (z_6) to a constant value $-\frac{\mathcal{K}}{k_3}$ and further $z_7 = u_2 = 0$.

When the robot is aligned with the line $z_3 = 0$ and $z_4 = 0$, the subsystem (13c) can be written as

$$\dot{z}_2 = z_5$$
$$\dot{z}_5 = \frac{(\sin 2z_6)(-b_5^2 g) + 2b_2 b_5 z_7^2 \sin z_6}{2(b_2 b_3 - b_5^2 \cos^2 z_6)} + \frac{b_2 + R b_5 \cos z_6}{b_3 R + b_5 \cos z_6} \times \left(\frac{\sin 2z_6(-b_5^2 z_7^2) + 2b_5 b_3 g \sin z_6}{2(b_2 b_3 - b_5^2 \cos^2 z_6)} - u_2 \right) \tag{22}$$

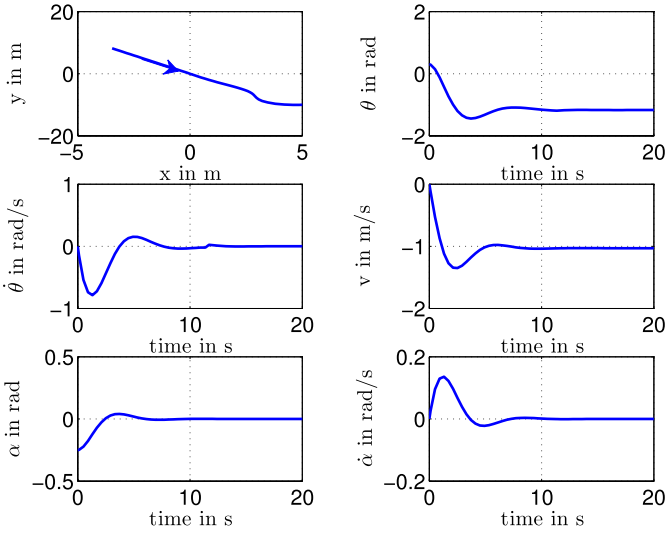

Fig. 7. Response for homing control when the MIP is in quadrant IV.

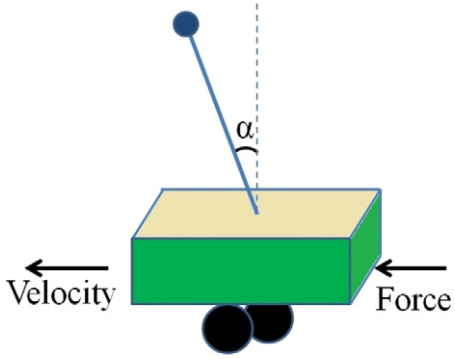

Fig. 8. Side view of pedaling action of MIP.

and together with the pendulum stabilized to $-\frac{\mathcal{K}}{k_3}$ using the controller (21), it becomes

$$\dot{z}_2 = z_5$$
$$\dot{z}_5 = \frac{(\sin 2z_6)(-b_5^2 g)}{2(b_2 b_3 - b_5^2 \cos^2 z_6)} + \frac{b_2 + R b_5 \cos z_6}{b_3 R + b_5 \cos z_6} \left(\frac{2b_5 b_3 g \sin z_6}{2(b_2 b_3 - b_5^2 \cos^2 z_6)} \right) = \frac{b_5 g \sin z_6}{b_3 R + b_5 \cos z_6}. \tag{23}$$

Case-1

If $\mathcal{K} > 0 \Rightarrow z_6 < 0$ and hence $\dot{z}_5 < 0$, which results in deceleration of the MIP.

Case-2

If $\mathcal{K} < 0 \Rightarrow z_6 > 0$ and hence $\dot{z}_5 > 0$, which results in acceleration of the MIP.

From case-1 and case-2, it is observed that the pendulum angle z_6 can be used as a pedal to force the MIP to move in the direction of z_6.

3.4. Moving toward the target

Our objective is to move the MIP from any arbitrary initial position toward the origin. The pedaling action explained in Section 3.3 is used to modify the pendulum stabilizing control law (17b) to move the robot toward the origin. This is equivalent to crossing the point ($z_2 = 0$). Since z_3 is made zero through the

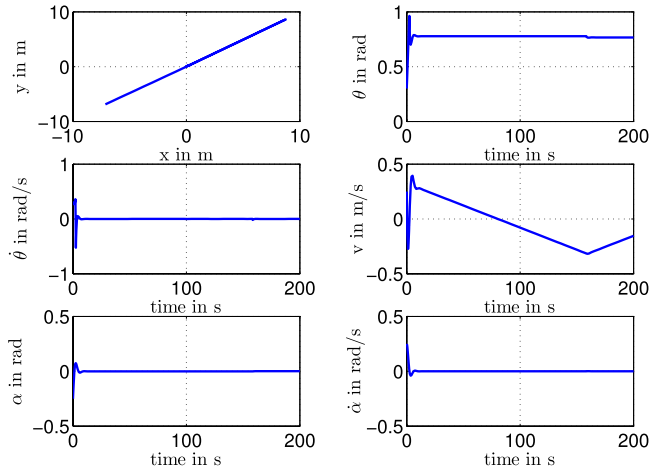

Fig. 9. Response for moving toward the target when the MIP is in quadrant I.

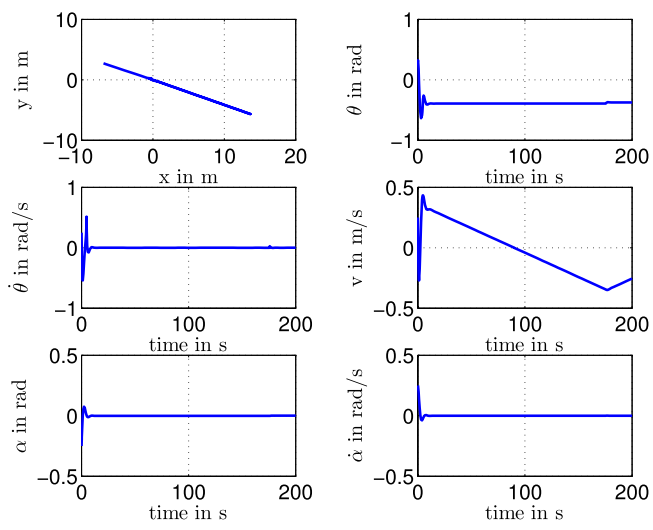

Fig. 10. Response for moving toward the target when the MIP is in quadrant II.

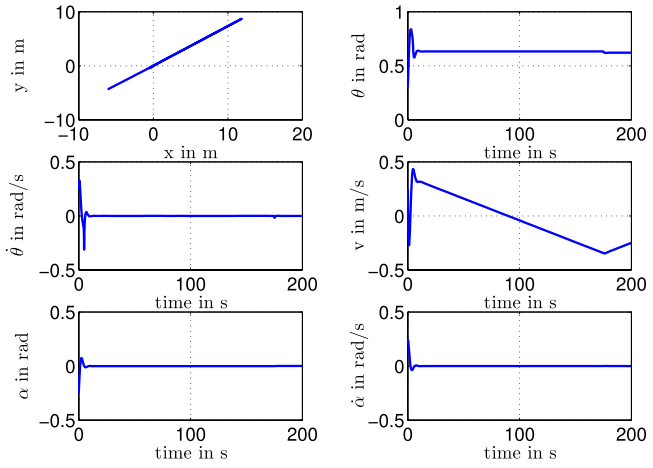

Fig. 11. Response for moving toward the target when the MIP is in quadrant III.

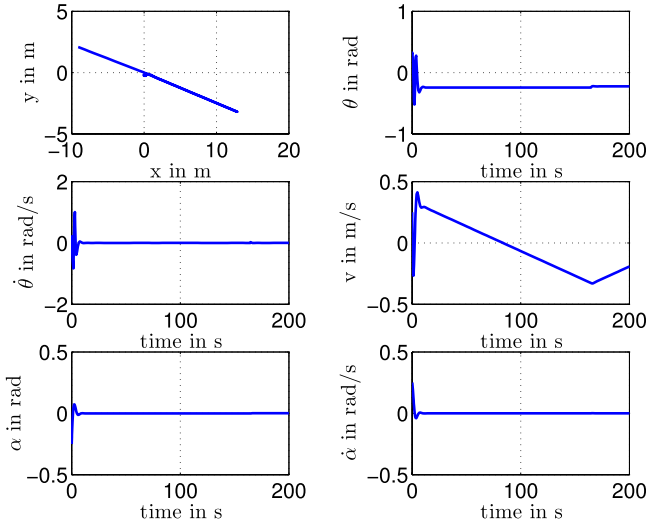

Fig. 12. Response for moving toward the target when the MIP is in quadrant IV.

homing control, making $z_2 = 0$ results in moving the robot to the origin in x–y plane.

This section explains about the modification made to the pendulum stabilizing controller such that the robot move toward the target point (cross the origin in x–y plane). Consider the case where $z_2 > 0$. To move the MIP toward the target point (the origin), the vehicle has to decelerate or $\dot{z}_5 < 0$. This can be achieved if the pendulum angle is set to a negative value by setting $\mathcal{K} > 0$ in (21). So the control law can be modified as

$$u_2 = -k_3 z_6 - k_4 z_7 - k_5 \text{sign}(z_2), \tag{24}$$

such that it will drive the MIP to the target position. This is simulated and the results are shown in Figs. 9–12.

3.5. Stopping at the target point

The modified control law (24) assures that, the robot move toward the origin but it will not stop. So, further the control law is modified to stop the robot at the target point.

Assume that the MIP is aligned with the line $z_3 = 0$ and the pendulum angle z_6 is regulated to zero, the subsystem (13c) becomes

$$\begin{aligned} \dot{z}_2 &= z_5 \\ \dot{z}_5 &= 0. \end{aligned} \tag{25}$$

The subsystem (25) can be stabilized only if z_2 and z_5 are of opposite signs and it ensures a stable region $\mathcal{R} = \{z_2, z_5 : z_2 z_5 < 0\}$ in the z_2–z_5 plane.

Now consider the control law

$$u_2 = -k_3 z_6 - k_4 z_7 - k_5 \text{sign}(z_2) - \mathcal{C} \tag{26}$$

where $|k_5| = |\mathcal{C}|$.

Case-1

If $z_2 > 0$, $\mathcal{C} < 0$ in (26) and the motion of the robot in $z_3 = 0$ line will make the pendulum angle z_6 to zero, which results in (25). At this instant $z_5 < 0$ causes a stabilizing motion at a constant velocity toward $z_2 = 0$ line. Whenever the MIP crosses the line $z_2 = 0$ and the instant at which z_2 becomes positive the pendulum angle is set to a positive constant value $(k_5 + \mathcal{C})$, which acts as a pedal and pushes the robot back to $z_2 = 0$ line. The above mentioned actions will be taking place whenever the MIP crosses the $z_2 = 0$ line and the robot will be pushed toward $z_2 = 0$ line. This aids the robot to settle in $z_2 = z_3 = 0$, which means the MIP has reached $x = y = 0$ in the original co-ordinates. The similar motion which always pushes the robot toward $z_2 = 0$ line will also happen for $z_2 < 0$, $\mathcal{C} > 0$.

Case-2

If $z_2 < 0$, $\mathcal{C} < 0$ in (26) and the motion of the robot is in $z_3 = 0$ line, the pendulum is set to a positive constant value $k_5 + \mathcal{C}$ which results in an acceleration pedal against the negative value of z_2 and causes a motion toward $z_2 = 0$ line and the MIP will cross the

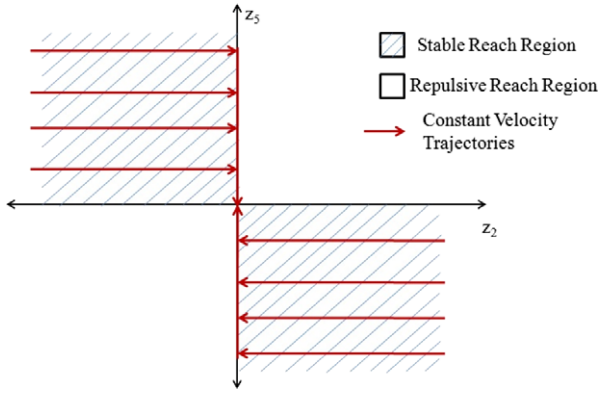

Fig. 13. Stable reach and repulsive reach region in z_2–z_5 plane.

point $z_2 = z_3 = 0$ and hence z_2 becomes positive. The robot can be pushed back to the point ($z_2 = z_3 = 0$), if we make $\mathcal{C} > 0$ at the instant z_2 becomes positive. This sets the pendulum angle z_6 to a negative constant value $-(k_5 + \mathcal{C})$ against the positive z_2 which results in a deceleration pedal.

From case-1 and case-2, it is observed that the value of $\mathcal{C}$ plays a major role in stabilizing the MIP at $z_2 = z_3 = 0$ and similar motion control can be obtained if we make $\mathcal{C} = k_6 \text{sign}(z_5)$ in (26).

The consequence of control law

$$u_2 = -k_3 z_6 - k_4 z_7 - k_5 \text{sign}(z_2) - k_6 \text{sign}(z_5) \tag{27}$$

on the stabilization of (13c) is depicted in Fig. 13. The quadrants II and IV in z_2–z_5 plane represent a stable reach region since z_2, z_5 have opposite signs which stabilize (25) and the system navigates at a constant velocity and reaches the point $x = y = 0$. At the same time in quadrants I and III the controller (26) acts as a pedal to stabilize the MIP.

Now, the integrated controller which performs homing, moving toward the target and stopping at the target in a required orientation is

$$\begin{aligned} u_1 &= -k_1(z_1 - z_{1r}) - k_2 z_4 \\ u_2 &= -k_3 z_6 - k_4 z_7 - k_5 \text{sign}(z_2) - k_6 \text{sign}(z_5) \end{aligned} \tag{28}$$

where $k_1,\ k_2,\ k_3,\ k_4,\ k_5,\ k_6 \in R$ are positive controller gains.

This controller moves all the state trajectories toward the origin. The velocity is regulated to a very small value based on the value of k_5. This velocity can be reduced even to zero in a practical system with the aid of inherent friction in the system.

The torque inputs given to the two motors attached to the left and right wheels using the controller (28) is,

$$\begin{aligned} \tau_r &= \frac{R}{4(b_3 R + b_5 \cos\alpha)}[\sin 2\alpha(b_3 b_1 \dot\theta^2 - b_5^2 \dot\alpha^2 \\ &\quad + 2b_3 b_5 g \sin\alpha) - 2(-k_3\alpha - k_4\dot\alpha + k_5 \text{ sign}(x\cos\theta \\ &\quad + y\sin\theta) + k_6 \text{ sign}(v))(b_2 b_3 - b_5^2\cos^2\alpha)] \\ &\quad + \frac{R}{2b}\left((-k_1(\theta - \theta_{1r}) - k_2\dot\theta)(b_4 \right. \\ &\quad \left. + b_1 \sin^2\alpha) + b_1\dot\theta\dot\alpha \sin 2\alpha\right) \\ \tau_l &= \frac{R}{4(b_3 R + b_5 \cos\alpha)}[\sin 2\alpha(b_3 b_1 \dot\theta^2 - b_5^2 \dot\alpha^2 \\ &\quad + 2b_3 b_5 g \sin\alpha) - 2(-k_3\alpha - k_4\dot\alpha + k_5 \text{ sign}(x\cos\theta \\ &\quad + y\sin\theta) + k_6 \text{ sign}(v))(b_2 b_3 - b_5^2\cos^2\alpha)] \\ &\quad - \frac{R}{2b}\left((-k_1(\theta - \theta_{1r}) - k_2\dot\theta)(b_4 \right. \\ &\quad \left. + b_1 \sin^2\alpha) + b_1\dot\theta\dot\alpha \sin 2\alpha\right). \end{aligned} \tag{29}$$

The closed loop equations of the system with the controller (28) is given by,

$$\begin{aligned} \dot x &= v\cos\theta \\ \dot y &= v\sin\theta \\ \ddot\theta &= -\frac{b_1\dot\alpha\dot\theta\sin 2\alpha}{b_4 + b_1\sin^2\alpha} + \frac{b}{R(b_4 + b_1\sin^2\alpha)}(\tau_r - \tau_l) \\ \dot v &= \frac{(\sin 2\alpha)(-b_1 b_5\dot\theta^2\cos\alpha - b_5^2 g) + 2b_2 b_5\dot\alpha^2\sin\alpha}{2(b_2 b_3 - b_5^2\cos^2\alpha)} \\ &\quad + \frac{b_2 + Rb_5\cos\alpha}{R(b_2 b_3 - b_5^2\cos^2\alpha)}(\tau_r + \tau_l) \\ \ddot\alpha &= \frac{\sin 2\alpha(b_3 b_1\dot\theta^2 - b_5^2\dot\alpha^2) + 2b_5 b_3 g\sin\alpha}{2(b_2 b_3 - b_5^2\cos^2\alpha)} \\ &\quad - \frac{b_3 R + b_5\cos\alpha}{R(b_2 b_3 - b_5^2\cos^2\alpha)}(\tau_r + \tau_l). \end{aligned}$$

This closed loop system can perform the tasks such as homing, moving toward the target, rotating to the desired orientation and then stopping at the desired location sequentially, while stabilizing the pendulum.

3.6. Stability analysis

Consider the internal dynamics (11)

$$\begin{aligned} \dot z_1 &= 0 \\ \dot z_2 &= z_5 \\ \dot z_5 &= 0 \end{aligned} \tag{30}$$

with the output considered as in (9). This results in $u_2 = 0$ and substituting this in (28), we obtain that

$$\text{sign}(z_2) = -\frac{k_6}{k_5}\text{sign}(z_5). \tag{31}$$

Also, the controller u_1 in (28) regulates z_1 to z_{1r} and z_3 to zero. Now, the internal dynamics of MIP using (28) results in

$$\begin{aligned} \dot z_1 &= 0 \\ \dot z_2 &= z_5 \\ \dot z_5 &= 0. \end{aligned} \tag{32}$$

Now, consider the Lyapunov candidate function

$$V = \frac{1}{2}z_1^2 + \frac{1}{2}z_2^2 + \frac{1}{2}z_5^2 \tag{33}$$

and its derivative is

$$\begin{aligned} \dot V &= z_1\dot z_1 + z_2\dot z_2 + z_5\dot z_5 \\ &= z_2\dot z_2 \\ &= z_2 z_5 \\ &= |z_2|\text{sign}(z_2)z_5. \end{aligned} \tag{34}$$

Substituting (31) in (34)

$$\begin{aligned} \dot V &= |z_2|\left(-\frac{k_6}{k_5}\text{sign}(z_5)\right)z_5 \\ &= -\frac{k_6}{k_5}|z_2|\,|z_5|. \end{aligned} \tag{35}$$

Since $\dot V$ in (35) is negative semi-definite, the stability can be proved through LaSalle's invariance principle [35].

When $\dot V = 0$

$z_2 = 0$

Table 2
System parameters.

Parameter	Value	Unit
M_b	3.9	kg
M_w	0.375	kg
R	0.1025	m
c_z	0.1	m
b	0.1620	m
g	9.8	N
I_x	0.02	kg m^2
I_y	0.015	kg m^2
I_z	0.01	kg m^2
I_w	0.002	kg m^2
I_{wa}	0.001	kg m^2

Table 3
Controller parameters.

Parameter	Value
k_1	1
k_2	1
k_3	1
k_4	1
k_5	0.001
k_6	0.001

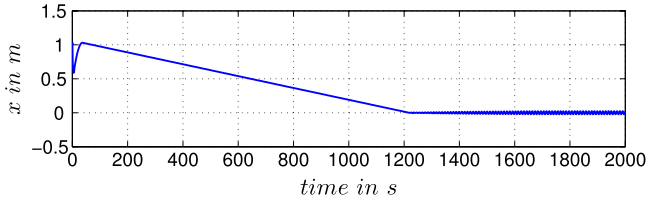

Fig. 14. Position in x direction.

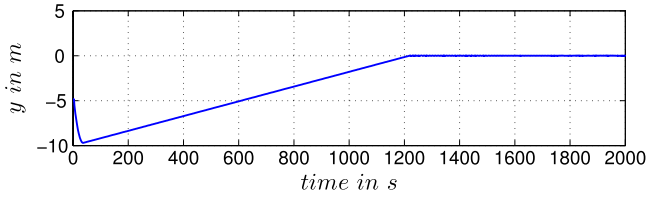

Fig. 15. Position in y direction.

and it implies that $\dot{z}_2 \equiv 0$ and from (32) we obtain that $z_5 \equiv 0$. Also, considering the case $\dot{V} = 0$ when $z_5 = 0$ will result in $z_2 = 0$. This can be proved using (31). Thus, it is proved that the controller (28) stabilizes the internal dynamics z_2, z_5 in (32) to zero. Also, $z_2 = z_3 = 0$ in (4), leads to $x = y = 0$ and substituting this condition in (16) makes $z_{1r}(t) = 0$. Also, $\dot{z}_4 = u_1 = 0$ implies that $z_1 = z_{1r}(t) = 0$ which leads to the stabilization of the system (7) to the equilibrium.

4. Simulation results

In this section, simulation results of the MIP using the proposed controller is presented. Table 2 shows the system parameters, which are chosen from [25], since it uses a heavier mass in the pendulum. All the simulations were carried out for a non zero initial condition. The response for homing control (17) for a non zero initial condition when the MIP is in quadrants I–IV of x–y plane is depicted in Figs. 4–7. The results shows that the controller is able to orient the robot toward the target in a finite time. The results for moving toward the target for all the four quadrants is shown in Figs. 9–12. These results show that the controller has the capability to move the robot to the origin. Finally, the motion tasks

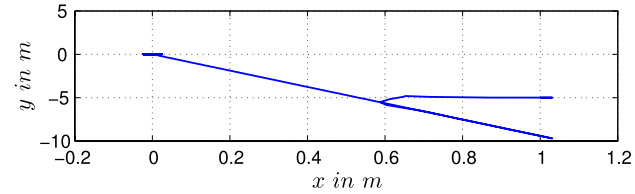

Fig. 16. Position in x–y plane.

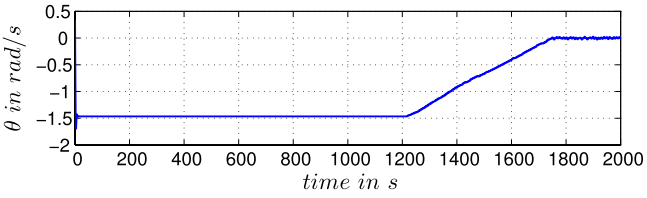

Fig. 17. Orientation of MIP (θ).

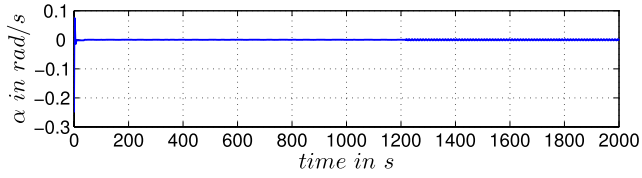

Fig. 18. Pendulum angle (α).

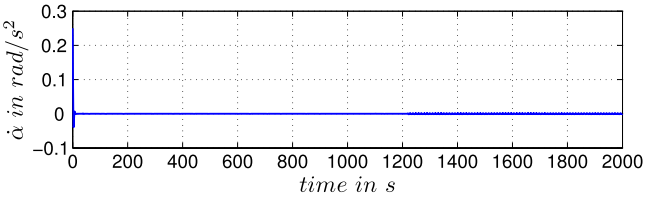

Fig. 19. Velocity of pendulum angle ($\dot{\alpha}$).

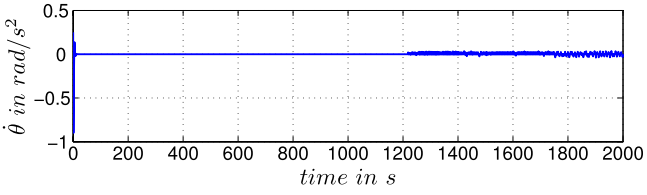

Fig. 20. Angular velocity of orientation angle ($\dot{\theta}$).

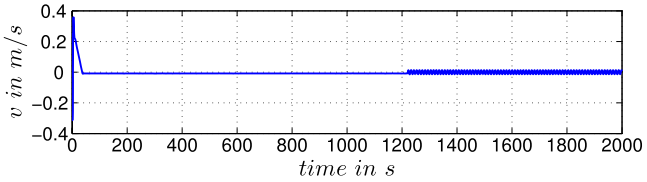

Fig. 21. Linear velocity (v).

such as targeting, moving toward the origin and stopping at the target in a required orientation are obtained by the controller (28) with the parameters as in Table 3 and the responses are given for the initial conditions $x(0) = 1$, $y(0) = -5$, $\theta(0) = 0.3$, $\dot{\theta}(0) = 0.25$, $v(0) = 0.25$, $\alpha(0) = -0.25$, $\dot{\alpha}(0) = 0.25$ in Figs. 14–25.

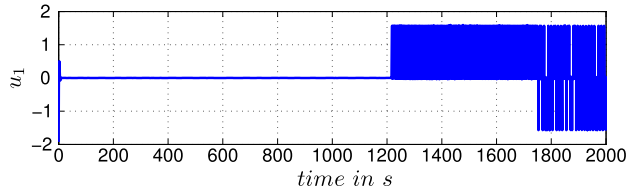

Fig. 22. Control input u_1.

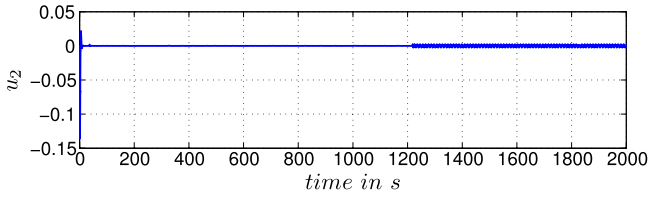

Fig. 23. Control input u_2.

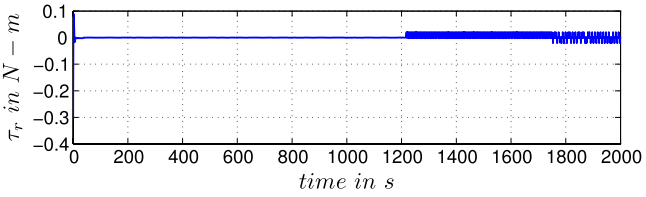

Fig. 24. Torque input to right wheel (N m).

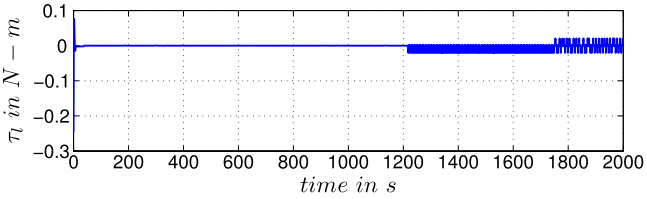

Fig. 25. Torque input to left wheel (N m).

5. Conclusion

A nonlinear controller is proposed to stabilize the mobile inverted pendulum to its equilibrium point. The proposed method does not demand for any switching between controllers when compared to the existing control techniques. It is proved that the internal dynamics of the closed loop system is stable. Simulations with realistic data show that, the proposed control strategy is effective.

References

[1] Y.-S. Ha, S. Yuta, Trajectory tracking control of the inverse pendulum type self-contained mobile robot, Robot. Auton. Syst. 17 (1–2) (1996) 65–80.
[2] Dean L. Kamen, J. Douglas Field, John B. Morrell, US6779621 B2, August 24, 2004.
[3] F. Grasser, A.D. Arrigo, S. Colombi, A.C. Rufer, JOE: A mobile, inverted pendulum, IEEE Trans. Ind. Electron. 49 (1) (2002) 107–114.
[4] R.W. Brockett, Asymptotic stability and feedback stabilization, in: Differential Geometric Control Theory, Birkhäuser, 1983, pp. 181–191.
[5] X. Yun, Y. Yamamoto, Internal dynamics of a wheeled mobile robot, in: IEEE/RSJ International Conference on Intelligent Robots and Systems, Yokohama, Japan, July 1993, pp. 1288–1294.
[6] K. Pathak, J. Franch, S.K. Agrawal, Velocity and position control of a wheeled inverted pendulum by partial feedback linearization, IEEE Trans. Robot. 21 (3) (2005) 505–513.
[7] O. Boubaker, The inverted pendulum benchmark in nonlinear control theory: A survey, Int. J. Adv. Robot. Syst. 10 (2013) 1–9.
[8] S.W. Nawawi, M. Ahmad, J.H.S. Osman, Development of a two-wheeled inverted pendulum mobile robot, in: The 5th Student Conference on Research and Development -SCOReD 2007, Malaysia, December 2007, pp. 1–7.
[9] M.T. Kang, H.D. Vo, H.K. Kim, S.B. Kim, Control system design for a mobile inverted pendulum via sliding mode technique, in: Proceedings of International Conference on Mechatronics, Kumamoto Japan, May 2007, pp. 1–6.
[10] J. Huang, H. Wang, T. Matsuno, T. Fukuda, K. Sekiyama, Robust velocity sliding mode control of mobile wheeled inverted pendulum systems, in: IEEE International Conference on Robotics and Automation, Kobe International Conference Center Kobe, Japan, May 2009, pp. 2983–2988.
[11] T. Nomura, Y. Kitsuka, H. Suemitsu, T. Matsuo, Adaptive backstepping control for a two-wheeled autonomous robot, in: ICROS-SICE International Joint Conference 2009, Fukuoka International Congress Center, Japan, August 2009, pp. 4687–4692.
[12] M.T. Ravichandran, A.D. Mahindrakar, Robust stabilization of a class of under-actuated mechanical systems using time-scaling and Lyapunov redesign, IEEE Trans. Ind. Electron. 58 (9) (2011) 4299–4313.
[13] W.-J. Chang, C.-H. Chang, C.-C. Ku, Fuzzy control with relaxed nonquadratic stability conditions for inverted pendulum robot system with multiplicative noise, in: 8th IEEE International Conference on Control and Automation, Xiamen, China, June 2010, pp. 1019–1024.
[14] J. Yi, N. Yubazaki, Stabilization fuzzy control of inverted pendulum systems, Artif. Intell. Eng. 14 (2000) 153–163.
[15] S. Jung, S.S. Kim, Control experiment of a wheel-driven mobile inverted pendulum using neural network, IEEE Trans. Control Syst. Technol. 16 (2) (2008) 297–303.
[16] T. Takei, R. Imamura, S. Yuta, Baggage transportation and navigation by a wheeled inverted pendulum mobile robot, IEEE Trans. Ind. Electron. 56 (10) (2009) 3985–3994.
[17] Z.L.C. Yang, Neural-adaptive output feedback control of a class of transportation vehicles based on wheeled inverted pendulum models, IEEE Trans. Control Syst. Technol. 20 (6) (2012) 1583–1591.
[18] C. Yang, Z. Li, R. Cui, B. Xu, Neural network-based motion control of underactuated wheeled inverted pendulum models, IEEE Trans. Neural Netw. Learn. Syst. 25 (11) (2014) 2004–2016.
[19] C.-H. Chiu, Y.-F. Peng, Y.-W. Lin, Intelligent backstepping control for wheeled inverted pendulum, Expert Syst. Appl. 38 (2011) 3364–3371.
[20] C.-H. Chiu, Y.-W. Lin, C.-H. Lin, Real-time control of a wheeled inverted pendulum based on an intelligent model free controller, Mechatronics 21 (2011) 523–533.
[21] Z. Li, C. Xu, Adaptive fuzzy logic control of dynamic balance and motion for wheeled inverted pendulums, Fuzzy Sets and Systems 160 (2009) 1787–1803.
[22] H.-C. Lu, M.-H. Chang, C.-H. Tsai, Adaptive self-constructing fuzzy neural network controller for hardware implementation of an inverted pendulum system, Appl. Soft Comput. 11 (2011) 3962–3975.
[23] A. Siuka, M. Schöberl, Applications of energy based control methods for the inverted pendulum on a cart, Robot. Auton. Syst. 57 (2009) 1012–1017.
[24] J. Huang, Z.-H. Guan, T. Matsuno, T. Fukuda, K. Sekiyama, Sliding-mode velocity control of mobile-wheeled inverted-pendulum systems, IEEE Trans. Robot. 26 (4) (2010) 750–758.
[25] V. Muralidharan, A.D. Mahindrakar, Position stabilization and waypoint tracking control of mobile inverted pendulum robot, IEEE Trans. Control Syst. Technol. 22 (6) (2014) 2360–2367.
[26] N. Adhikary, C. Mahanta, Integral backstepping sliding mode control for underactuated systems: Swing-up and stabilization of the cart-pendulum system, ISA Trans. 52 (2013) 870–880.
[27] Z.-Q. Guo, J.-X. Xu, T.H. Lee, Design and implementation of a new sliding mode controller on an underactuated wheeled inverted pendulum, J. Franklin Inst. B 351 (2014) 2261–2282.
[28] R.P.M. Chan, K.A. Stol, C.R. Halkyard, Review of modelling and control of two-wheeled robots, Annu. Rev. Control 37 (2013) 89–103.
[29] F. Gordillo, J. Aracil, A new controller for the inverted pendulum on a cart, Internat. J. Robust Nonlinear Control 18 (17) (2008) 1607–1621.
[30] B. Srinivasan, P. Huguenin, D. Bonvin, Global stabilization of an inverted pendulum—control strategy and experimental verification, Automatica 45 (2009) 265–269.
[31] K.Y. Petterson, O. Egeland, Exponential stabilization of an underactuated surface vessel, in: Proceedings 35 th IEEE Conference on Decision and Control, 1996, pp. 967–972.
[32] J.-J.E. Slotine, W. Li, Applied Nonlinear Control, Prentice Hall, Englewood Cliffs, New Jersey, 1991.
[33] A.D. Luca, Nonlinear synthesis, in: proceedings of IIASA workshop held in Sapron, Hungary, June 1989, pp. 68–87.
[34] V. Sankaranarayanan, A.D. Mahindrakar, Switched control of a nonholonomic autonomous mobile robot, Commun. Nonlinear Sci. Numer. Simul. 14 (2009) 2319–2327.
[35] H.K. Khalil, Nonlinear Systems, third ed., Prentice-Hall. Inc., Pearson Education International, Upper Saddke River, New Jersy, 1996.